Plastic-deformation behavior of steel pipe piles based on large-deformation lateral-loading tests

T. Kobayashi
Researcher, Steel Structures Research Laboratories, Nippon Steel Corporation, Chiba, Japan
Y. Ishihama
Chief Researcher, Steel Structures Research Laboratories, Nippon Steel Corporation, Chiba, Japan
H. Kashiwa
Professor, Division of Global Architecture, Osaka University, Osaka, Japan

ABSTRACT

It is necessary to clarify the seismic performance of pile foundations against large earthquakes, considering the damage caused by previous earthquakes and the predicted severity of future seismic motions. Steel pipe piles exhibit excellent plastic-deformation capacity and high seismic resistance. However, cases where steel pipe piles are horizontally loaded up to the large-deformation range have not been investigated, in which the strength decreases owing to local buckling in a pile-soil system, and the seismic performance at that region is unknown. Therefore, in this study, large-deformation lateral-loading tests were performed on steel pipe piles driven into the in-situ ground, in which a horizontal force was applied up to the ultimate limit state where local buckling occurs, and the strength decreases. In addition, the plastic-deformation behavior of the steel pipe piles was analyzed. The results reveal the following. 1) The ultimate strain ε_u (= $0.44t/D$) evaluates the local-buckling strain of the steel pipe piles in the pile-soil system on the safe side. 2) In a pile-soil system, steel pipe piles maintain loads up to a high ductility factor, as the diameter-thickness ratio D/t is lower, and exhibits plastic-deformation performance equivalent to or better than that in air. 3) The pile characteristic value influences the plastic-deformation behavior of steel pipe piles and the energy sharing between the pile and the soil. 4) As the horizontal displacement of the pile head increases, the energy sharing between the pile and the soil tends to converge to a constant value.

Key words: *steel pipe piles, lateral-loading test, plastic deformation, energy absorption*

1. Introduction

Clarifying the seismic performance of pile foundations against large earthquakes is necessary, considering the damage of pile foundations caused by recent large earthquakes and the predicted severity of future seismic motions. Elucidating the plastic-deformation and energy-absorption behaviors of pile foundations up to the ultimate limit state will facilitate the development of more reliable and rational seismic-resistant design methods and construction of seismic-resistant structures.

Because steel pipe piles exhibit excellent plastic-deformation capacity, high seismic resistance performance can be expected. The following are examples of previous studies in which steel pipe piles were horizontally loaded up to a displacement where they become plastic in the pile-soil system. Ogasawara et al. (1991) performed lateral-loading tests on a single steel pipe pile in the in-situ ground and found that the plasticity of the steel pipe pile occurred after the soil plasticity progressed. For lateral-loading tests on single and grouped steel pipe piles in in-situ soil, Aoto et al. (2001) applied unidirectional and cyclic loadings up to a pile head horizontal displacement of approximately 80% of the pile diameter, with the number of piles and pile arrangement as the parameters. They observed that the loading method minimally influenced the relationship between the pile-head horizontal load and the pile-head horizontal displacement. Kurata et al. (2007) and Kashiwa et al. (2008) conducted cyclic lateral-loading tests in which a large amplitude of up to three times the pile diameter was applied to a group of model steel pipe piles. They also analyzed the plastic-deformation behaviors of the piles and soil. However, in these studies, loads were not applied up to the large-deformation region, such as where local buckling of steel pipe piles occurs and where the strength of the pile-soil system decreases. Furthermore, the plastic-deformation behavior of steel pipe piles up to this region and the energies absorbed by the pile and soil have not been investigated in detail.

In this study, large-deformation lateral-loading tests were performed for steel pipe piles driven into the in-situ soil, in which a horizontal force was applied up to the ultimate limit state, where local buckling occurs and the strength decreases. The plastic-deformation behavior of the steel pipe piles in the pile-soil system was assessed. In addition, energy absorption was analyzed as the seismic performance of the steel pipe piles.

2. Test conditions

2.1. Test pile

Table 1 lists the test pile specifications. The test pile was a steel pipe pile (STK400). Three cases were investigated using pile diameters D of 101.6 and 216.3 mm and diameter-thickness ratios D/t of approximately 25 and 50 as the parameters. Tensile tests were conducted on specimens taken axially from each test pile, and the yield point σ_y and tensile strength σ_t were determined. The pile was installed in the in-situ soil using a driving method. The pile was driven to an embedded depth of 5 m to satisfy the semi-infinite length pile conditions (**Eq. (1)** and **(2)**) (Chang, 1937):

$$\beta L \geq 3 \tag{1}$$

$$\beta = \sqrt[4]{\frac{k_h D}{4EI}} \tag{2}$$

where β is the characteristic value of the pile (1/m), L is the embedded length (m), k_h is the horizontal ground reaction force coefficient (kN/m^3), E is the Young's modulus of the pile (kN/m^2), and I is the moment of inertia of the pile (m^4).

Table 1 Test pile conditions

Case	Pile diameter D (mm)	Thickness t (mm)	Diameter-thickness ratio D/t	Yield point σ_y (N/mm^2)	Tensile strength σ_t (N/mm^2)	Yield ratio σ_y/σ_t (%)
Case1	101.6	4.2	24.2	388	461	84.1
Case2	216.3	8.2	26.4	405	487	83.2
Case3	216.3	4.5	48.1	346	443	78.0

2.2. Ground conditions

Fig. 1 shows representative data of the cone penetration test (CPT) as ground conditions of the in situ ground. The converted standard penetration test (SPT) N was calculated using Suzuki's proposed formula (**Eq. (3)**) (Suzuki et al., 2003) based on the CPT result. The in-situ ground was mainly composed of sandy soil, and the converted SPT N within the driving depth of the steel pipe pile was lower than 15.

$$\begin{aligned}&(q_t > 0.2)\\&\text{Converted SPT } N = 0.341 {I_c}^{1.94}(q_t - 0.2)^{1.34-0.0927 I_c}\\&(q_t \leq 0.2)\\&\qquad \text{Converted SPT } N = 0\end{aligned} \tag{3}$$

where I_c is the soil properties index, and q_t is the corrected tip resistance (N/mm^2).

Evaluating the ground deformation coefficient E_0 (kN/m^2) by **Eq. (4)** and the horizontal ground reaction force coefficient k_h (kN/m^3) by **Eq. (5)**, the characteristic value of the pile β is 1.34 (1/m) in Case 1, 0.75 (1/m) in Case 2 and 0.86 (1/m) in Case 3.

$$E_0 = 700N \tag{4}$$

$$k_h = 80E_0(D/D_0)^{-3/4} \tag{5}$$

where D_0 is the reference value of pile diameter (=0.01m).

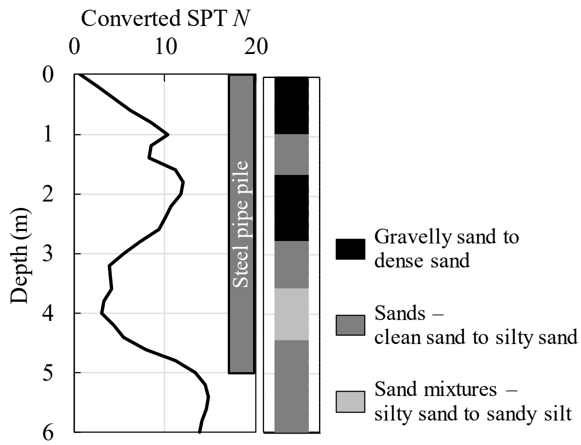

Fig. 1 Ground conditions

2.3. Loading and measurement methods

Fig. 2 shows the loading device. The test was conducted by applying a load in one horizontal direction at the pile head (GL.+150mm) under free rotation conditions. The experiment was performed up to a displacement where the steel pipe pile exhibited local buckling, and the horizontal load sufficiently decreased from its maximum value.

Fig. 3 shows the strain measurement positions. The strains generated in the pile were measured using a strain gauge affixed axially to the outer surface of the pile. In addition, the horizontal displacements of the pile at the pile head position (GL.+150mm) and near the ground surface (GL.+50mm) were measured using a displacement meter.

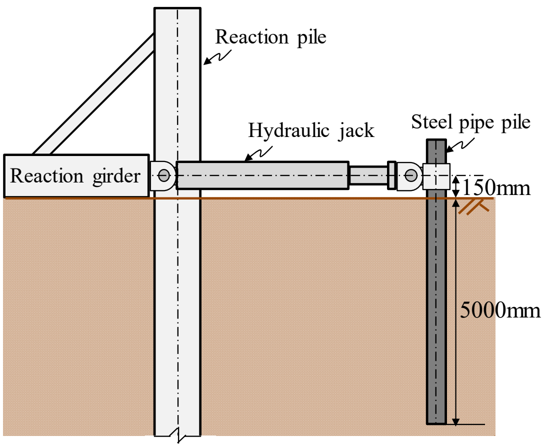

Fig. 2 Loading device

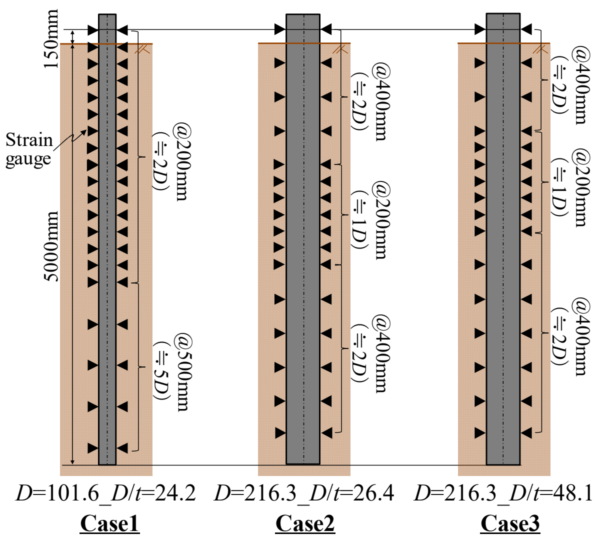

Fig. 3 Strain measurement positions

3. Test results and discussion

3.1. Plastic-deformation behavior

Fig. 4 shows the relationship between the pile-head horizontal load P and pile-head horizontal displacement δ. In **Fig. 4**, ●, ■, ▲, and ◆ represent the yield of the steel pipe pile, the ultimate strain, the maximum load, and the reduction to 95% of the maximum load, respectively. The yield was defined as the displacement caused to the pile by yield curvature ϕ_y, expressed by **Eq. (6)**, and the ultimate strain was defined as the displacement caused to the pile by ultimate curvature ϕ_u, expressed by **Eq. (7)**. The ultimate strain was the lower-limit value of the steel pipe strain at the maximum load for the buckling test results of circular steel pipes subjected to compressive axial force and stub-column compression test results of spiral steel pipes presented in the Recommendations for Design of Building Foundation (AIJ, 2019). The value is used to evaluate the local-buckling strain on the safe side.

$$\phi_y = 2\varepsilon_y / D \quad (6)$$

$$\phi_u = 2\varepsilon_u / D \quad (7)$$

where ε_y is the yield strain (= σ_y/E), and ε_u is the ultimate strain (= $0.44t/D$).

In all cases, the displacement gradually increased with loading until yielding of the pile occurred. As the plasticity of the pile progressed, the increase in displacement became more significant than the increase in the load, and the load decreased as the maximum load was reached, after the ultimate strain occurred.

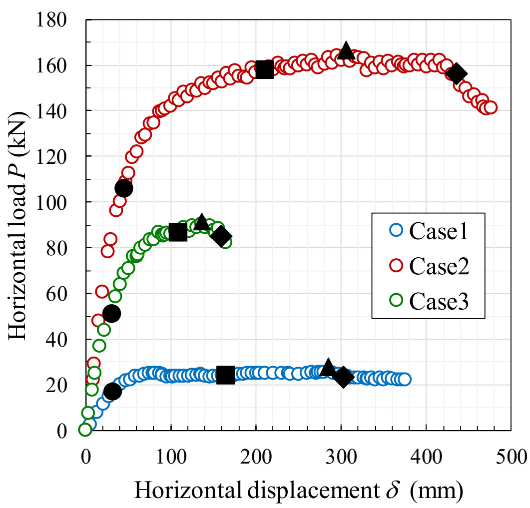

Fig. 4 Relationship between horizontal load and displacement

Fig. 5 shows the conditions of the test piles pulled out from the ground after the test. Local buckling was observed, and the decrease in load in the large-deformation region (**Fig. 4**) is assumed to be caused by local buckling. Thus, the test results confirmed that local buckling occurred in the steel pipe piles inside the ground, and the horizontal resistance of the pile-soil system decreased. In addition, in the pile-soil system, it was confirmed that the ultimate strain evaluates the local-buckling strain on the safe side.

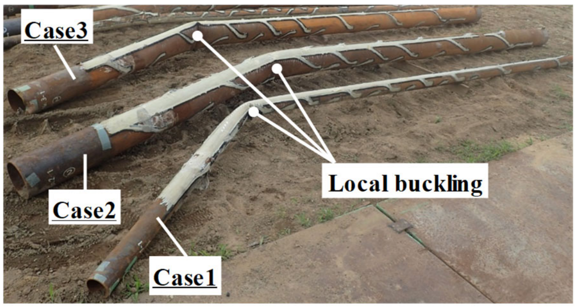

Fig. 5 Conditions of steel pipe piles after lateral-loading test

Fig. 6 shows the load-deformation relationship, based on **Fig. 5**, with the vertical axis normalized by yield load P_y and the horizontal axis normalized by yield displacement δ_y.

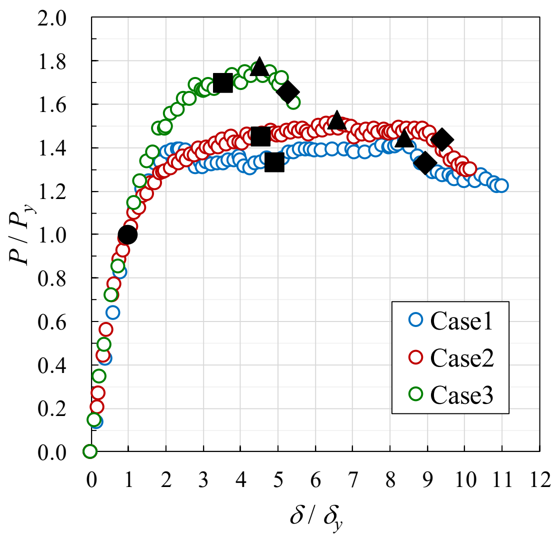

Fig. 6 Relationship between horizontal load and displacement (normalized)

Strength performance

The effect of the pile diameter on the strength performance was analyzed for Cases 1 and 2. The strength factors P/P_y at the maximum load were 1.43 and 1.51 in Cases 1 and 2, respectively, and both exhibited equivalent strength performance. Hence, the pile diameter is presumed to have a minimal effect on the strength performance of the pile-soil system.

The effect of the diameter-thickness ratio on the strength performance was analyzed for Cases 2 and 3. The strength factors P/P_y at the maximum load were 1.51 and 1.76 in Cases 2 and 3, respectively, and the case with a high diameter-thickness ratio exhibited high strength performance. This finding differs from those obtained for bending tests on steel pipes in air (for example, Tsuda et al., 1998), in which the higher the diameter-thickness ratio, the lower the strength performance. P/P_y at the maximum load in Case 3 exceeded that in Case 2 because of the effect of the yield ratio. As listed in **Table 1**, the yield ratio for Case 3 (78.0%) was lower than that for Case 2 (83.2%). Therefore, it is presumed that Case 3 exhibited significantly increased strength after the plasticity of the pile and showed high strength performance despite the high diameter-thickness ratio.

Deformation performance

The effect of the pile diameter on the deformation performance was analyzed for Cases 1 and 2. In both cases, the ductility factors δ/δ_y during the occurrence of the ultimate strain were approximately equivalent, whereas the subsequent behaviors differed. In other words, Case 1 yielded a high δ/δ_y value of 8.41 under the maximum load, and subsequently, the strength decreased early. The δ/δ_y value was 8.81 until the strength decreased to 95%, indicating a slight increase. However, although Case 2 exhibited a relatively low δ/δ_y of 6.53 at the maximum load, the strength was maintained subsequently, and the δ/δ_y value reached as high as 9.31 until the strength decreased to 95%. This is thought to be due to the following reasons. That is, in Case 1, in which the pile diameter was small, the pile had a high characteristic value β, so the shallow and relatively soft ground provides resistance, and the plasticity of the pile progresses gradually in response to the increase in displacement. Thus, a large displacement was required until the maximum strength was reached. In contrast, after the maximum strength was reached, the resistance share of the pile was large due to the softness of the ground, and it is presumed that the strength decreased early. In Case 2, in which the pile diameter was large, the pile had a low β value. Hence, by contributing to the resistance down to the deep and strong ground, the maximum strength was reached at a relatively small displacement, the resisting ability of the soil was retained, and the strength was subsequently maintained. Even if the diameter-thickness ratio is constant and only the pile diameter varies in a pile-soil system, it was experimentally confirmed that the ductility factor δ/δ_y that can maintain the load changes because of the variation in the β value of the pile.

The effect of the diameter-thickness ratio on the deformation performance was analyzed for Cases 2 and 3. The ductility factor δ/δ_y was larger in Case 2 than in Case 3 at the ultimate strain, maximum load, and 95% strength reduction. Thus, it was confirmed that in the pile-soil system, the smaller the diameter-thickness ratio, the greater the deformation performance. When D/t = 25, the δ/δ_y values were 4 or higher at the occurrence of the ultimate strain, 6 or higher at the maximum load, and 8 or higher at 95% strength reduction. When D/t = 50, the δ/δ_y values were 3 or higher at the ultimate strain, 4 or higher at the maximum load, and 5 or higher at 95% strength reduction. The Specifications for Highway Bridges (Japan Road Association, 2017) expects a ductility factor of about 4 for steel pipe piles to retain horizontal strength based on the results of horizontal loading tests of piles in air. However, the deformation performance of the steel pipe pile in the pile-soil system in this test exceeded that value.

3.2. Energy-absorption behavior

3.2.1. Method for calculating absorbed energy

A method for calculating the amounts of energy absorbed by the piles and soil is described. Assuming that the external work performed by forces applied to the pile head using a horizontal jack is equal to the internal work stored in the pile and soil, the evaluation is performed using **Eq. (8)**:

$$E_{all} = E_{pile} + E_{soil} \tag{8}$$

where E_{all} is the total amount of energy applied to the pile head using the horizontal jack (kNm), E_{pile} is the amount of energy absorbed by the pile (kNm), and E_{soil} is the amount of energy absorbed by the soil (kNm).

The detailed explanation of the energy calculation method is provided in **Fig. 7**. Energy is evaluated in a manner that includes elastic and plastic energy. E_{all} was calculated by integrating the horizontal load-displacement relationship determined from the values obtained from the load cell connected to the horizontal jack and from the horizontal displacement meter installed on the pile head part（**Fig. 7(a)**）. The results of the tensile tests conducted on specimens taken axially from each test pile and bilinear models are presented in **Fig. 8**. During the bilinear modeling of the stress-strain relationship, the yield point σ_y presented in **Table 1** was adopted as the breaking point. In addition, the first stiffness (initial stiffness) was 205,000 N/mm^2, and the second stiffness was 1/100 of the first stiffness based on the Recommendations for Design of Building Foundation (AIJ, 2019). E_{pile} was calculated by integrating the corresponding stresses in the bilinear modeled stress-strain relationship shown in **Fig. 8** over the entire length of the pile, based on the Bernoulli-Euler theory and using the measured values of strain gauges attached to the outer surface of the pile（**Fig. 7(b)**, **(c)**）. The burden length of each strain gauge was set by dividing it at the midpoint between the adjacent gauges in the axial direction（**Fig. 7(d)**）. Because plane retention could not be maintained when accompanied by cross-sectional deformation owing to local buckling, the energy was evaluated for up to the maximum load, which is considered to be less affected by the cross-sectional deformation. E_{soil} was calculated by subtracting E_{pile} from E_{all}.

3.2.2. Cumulative energy

Fig. 9 shows the transition of the cumulative energy. In **Fig. 9**, ●, ■, and ▲ represent the yield of the steel pipe pile, the ultimate strain, and the maximum load, respectively. In all cases, the E_{all}, E_{pile}, and E_{soil} values increased with increasing pile head horizontal displacement until the maximum load was reached.

The effect of the pile diameter on cumulative energy was analyzed for Cases 1 and 2. In Case 1, in which the pile diameter is small, E_{pile} tended to increase more steeply than E_{soil} after yielding of the pile. In contrast, in Case 2,

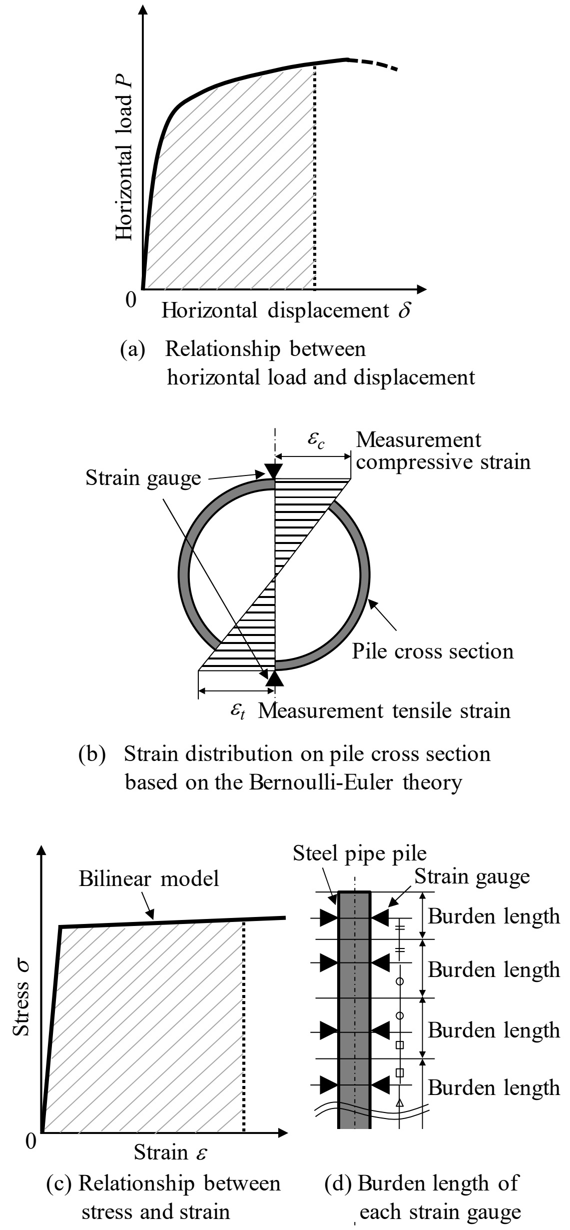

(a) Relationship between horizontal load and displacement

(b) Strain distribution on pile cross section based on the Bernoulli-Euler theory

(c) Relationship between stress and strain

(d) Burden length of each strain gauge

Fig. 7 Method for calculating the amounts of energy

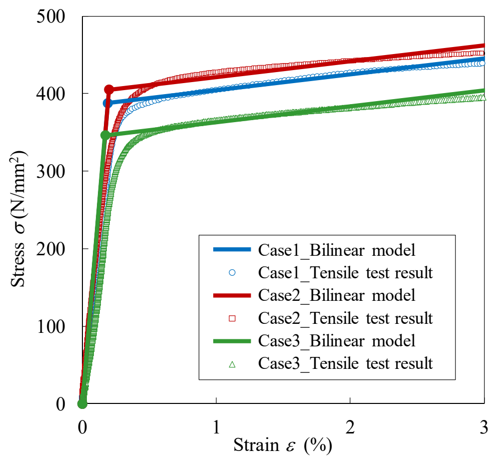

Fig. 8 Relationship between stress and strain

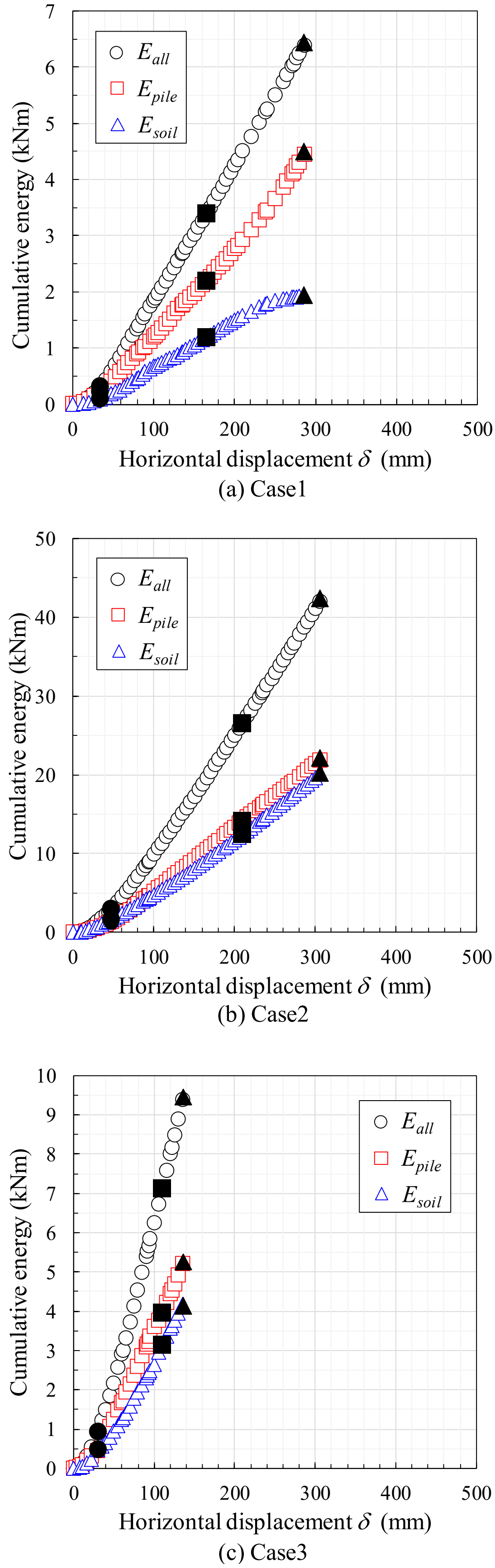

(a) Case1

(b) Case2

(c) Case3

Fig. 9 Relationship between cumulative energy and displacement in which the pile diameter is large, E_{pile} and E_{soil} increased at approximately the same slope. This is because when the pile diameter is small, the characteristic value β of the pile is high, and the range at which the soil deforms is relatively narrow; hence, E_{pile} was predominant. However, when the pile diameter is large, the β value is low, and soil deformation extends deeper and farther; thus, it is thought that E_{soil} became large and remained on par with E_{pile}. Therefore, it is suggested that the energy-absorption behavior of the pile and soil changes due to the different plasticization range of the soil caused by the change in β values depending on the difference in pile diameters.

The effect of the diameter-thickness ratio on cumulative energy was assessed for Cases 2 and 3. Although the pile head horizontal displacements at the maximum load differed significantly in both cases owing to the variation in deformation performance with diameter-thickness ratio, the increasing trends of E_{pile} and E_{soil} up to the maximum load were generally similar in both cases. Because the β values in Cases 2 and 3 differed, the ranges of the soil that contributed as resistance were different. However, at each displacement stage in both cases during the tests, the increases in E_{pile} (owing to the plastic deformation of the pile) and E_{soil} (owing to the expansion of the plastic region of the soil) were generally similar. Therefore, it is presumed that the influence of the diameter-thickness ratio was minimal.

3.2.3. Energy sharing between pile and soil

Fig. 10 shows the energy sharing between the pile and the soil. In **Fig. 10**, ●, ■, and ▲ indicate the yield of the steel pipe pile, the ultimate strain, and the maximum load, respectively. In all cases, the proportion of E_{pile} and E_{soil} generally converged with an increase in the pile head horizontal displacement, and the pile bore more than 50% of the energy at the ultimate strain and maximum load.

The effect of pile diameter on energy sharing between the pile and the soil was examined for Cases 1 and 2. In Case 1, in which the pile diameter was small, the ratio of E_{pile} was always higher than E_{soil}, and the pile bore more than 65% of the energy at the ultimate strain and maximum load. In Case 2, in which the pile diameter was large, the ratio of E_{soil} exceeded E_{pile} at the time of yielding of the pile, E_{pile} increased gradually, and the pile and soil each shared approximately 50% of the energy at the

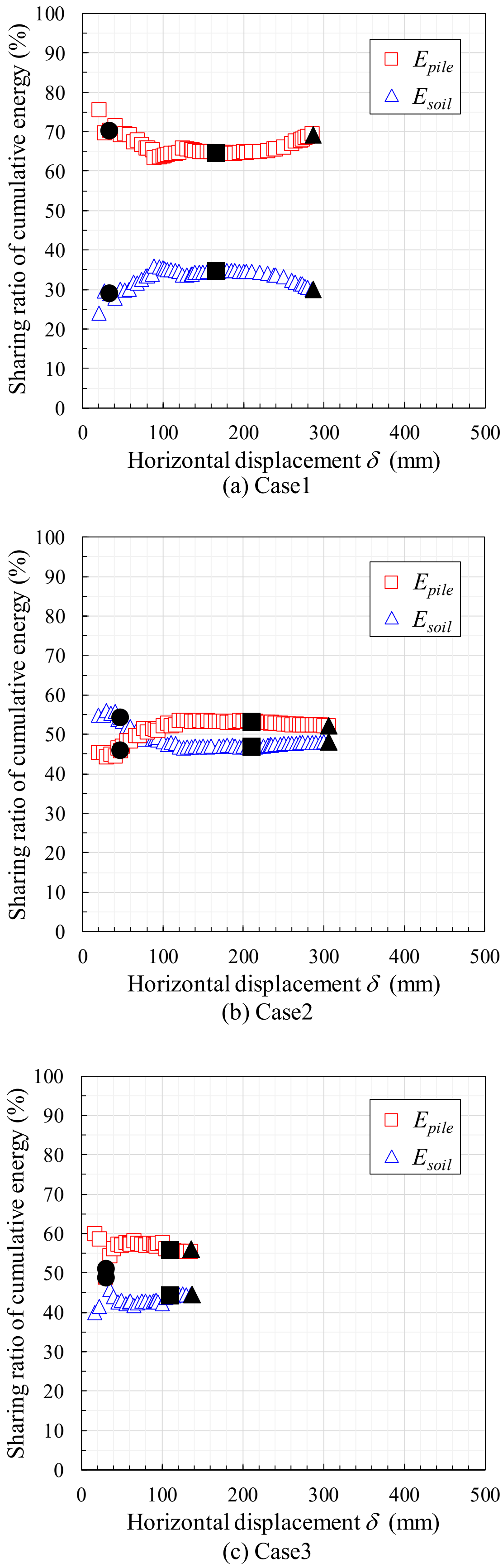

Fig. 10 Sharing ratio of cumulative energy

ultimate strain and maximum load. The larger ratio of E_{pile} in Case 1 compared to Case 2 is presumably due to the different β values, as discussed in Section **3.2.2**.

The effect of the diameter-thickness ratio on energy sharing between the pile and the soil was analyzed for Cases 2 and 3. Regardless of the diameter-thickness ratio, the final energy sharing between the pile and the soil was similar. This is presumably because of the reason explained in Section **3.2.2**.

4. Conclusion

In this study, large-deformation lateral-loading tests were conducted, in which horizontal forces were applied to steel pipe piles driven into the in-situ ground up to the ultimate limit state where local buckling occurred and the strength decreased. The plastic-deformation behavior and energy-absorption behavior of the steel pipe piles in the pile-soil system were analyzed. The conclusions of this study are as follows.

1) Local buckling of steel pipe piles occurs inside the ground, which decreases the horizontal load in the pile-soil system. The local-buckling strain is evaluated on the safe side by using the ultimate strain ε_u (= $0.44t/D$).
2) In the pile-soil system, the smaller the diameter-thickness ratio D/t, the more the steel pipe pile can sustain the load up to a larger ductility factor δ/δ_y and shows plastic-deformation performance equivalent or superior to that in air.
3) The characteristic value β of the pile influences the plastic-deformation behavior of the steel pipe piles and the energy sharing between the pile and the soil.
4) As the pile head horizontal displacement increases, the energy sharing between the pile and the soil tends to converge to a constant value. In all cases investigated in this experimental study, the pile bore more than 50% of the energy at the onset of the ultimate strain and at maximum load.

References

Aoto, K. et al., 2001. Lateral loading tests of steel group piles in the large deformation and its numerical simulation. Proceedings of the 46th geotechnical engineering symposium, pp.229-234.

Architectural Institute of Japan, 2019. Recommendations for Design of Building Foundation.

Japan Road Association, 2017. Specifications for Highway Bridges, Part IV Substructures.

Kashiwa, H. et al., 2008. Study on effect of nonlinear behavior of pile-soil system on displacement amplitude dependence of effect of pile group based on cyclic lateral loading tests subjected to large displacement. Journal of structural engineering, Vol.54B, pp.51-58.

Kurata, T. et al., 2007. Non-linear behavior of pile group-soil system based on horizontal loading test subject to large displacement. Journal of structural and construction engineering, No.614, pp.45-52.

Ogasawara, M. et al., 1991. Study on a loading capacity of pile foundation. Journal of structural engineering, Vol.37A, pp.1467-1477.

Suzuki, Y. et al., 2003. Correlations between CPT data and soil characteristics obtained from SPT. Journal of structural and construction engineering, No.566, pp.73-80.

Tsuda, K. et al., 1998. Inelastic behavior of circular steel tubular beam-columns under constant vertical and alternating horizontal loads. Journal of structural and construction engineering, No.505, pp.131-138.

Y. L. Chang, 1937. Lateral Pile-Loading Tests. Paper 1959, Trans. ASCE, Vol.102, pp.272-277